

## Synthesis, Properties and Self-Assembly of Intelligent Core-Shell Nanoparticles Based on Chitosan with Different Molecular Weight and *N*-Isopropylacrylamide

Yajing Wang,<sup>1</sup> Jiu Wang,<sup>1</sup> Liang Ge,<sup>1</sup> Qi Liu,<sup>1</sup> Liqun Jiang,<sup>1</sup> Jiabi Zhu,<sup>1</sup> Jianping Zhou,<sup>2</sup> Fei Xiong<sup>3</sup>

<sup>1</sup>Pharmaceutical Research Institute, China Pharmaceutical University, Nanjing, Jiangsu Province 210009, China

<sup>2</sup>Department of Pharmaceutics, China Pharmaceutical University, Nanjing, Jiangsu Province 210009, China

<sup>3</sup>State Key Laboratory of Bioelectronics, Jiangsu Laboratory for Biomaterials and Devices, School of Biological Science and Medical Engineering, Southeast University, Nanjing, Jiangsu Province 210009, China

Y. W. and J. W. contributed equally to this article.

Correspondence to: J. Zhu (E-mail: jiabizhu@yahoo.cn)

**ABSTRACT:** In this study, a series of chitosan-graft-poly(*N*-isopropylacrylamide) (CTS-g-PNIPAAm) copolymers based on different molecular weight (Mw) of CTS and NIPAAm were synthesized through the polymerization of NIPAAm in an acid aqueous solution. The structures were verified by Fourier transform infrared and nuclear magnetic resonance. The influence of the CTS Mw on the properties of the resulting copolymers and self-assembled nanoparticles was fully examined. The grafting ratio and grafting efficiency of the copolymers increased with the CTS Mw. All the copolymers have a similar low critical solution temperature of 33.5°C, which was independent of the CTS Mw. Furthermore, the copolymers were less temperature sensitive, when CTS Mw increased to 200 kDa. Besides, once the CTS Mw increased to 700 kDa, the copolymers were less pH sensitive near the tumor site (from pH 7.4 to 6.8). The copolymers could form uniform nanoparticles once the temperature increased to 34°C, which was reversible. After crosslinking by *N,N*-methylenebisacrylamide (MBA), structurally stable nanoparticles could be obtained. The results from Transmission electron microscope (TEM) and Atomic force microscopy (AFM) showed that the MBA crosslinked nanoparticles were uniformly spherical with a loose structure. Surface tension method indicated that the critical aggregate concentrations were 0.045, 0.042, 0.037, and 0.036 mg mL<sup>-1</sup> prepared from CTS 50, 100, 200, and 700 kDa, respectively. © 2012 Wiley Periodicals, Inc. *J. Appl. Polym. Sci.* 000: 000–000, 2012

**KEYWORDS:** stimuli-sensitive polymers; graft copolymers; crosslinking; self-assembly; molecular weight distribution/molar

Received 7 September 2011; accepted 6 March 2012; published online 00 Month 2012

**DOI:** 10.1002/app.37648

### INTRODUCTION

Double hydrophilic block copolymers (DHBCs), as a new class of amphiphilic block copolymers, have received considerable attention within the past decade due to their important and unique roles for the preparation of nanomaterials. Under a proper adjustment of external conditions such as pH, temperature, and so on, one of the blocks from DHBCs can be rendered insoluble, while the other block still remains soluble. Consequently, these copolymers are capable of supramolecularly self-assembling into colloid particles with various morphologies such as micelles, vesicles, or nanoparticles, and so on. This unique property makes DHBCs as a promising “intelligent” system for many applications such as drug delivery, coatings, interface mediators, catalysis, and so forth.<sup>1</sup>

Poly(*N*-isopropylacrylamide) (PNIPAAm) is one of the most popular thermoresponsive polymers, which shows dramatic and reversible phase transition behavior in water with the low critical solution temperature (LCST) at around 32°C.<sup>2</sup> Over the past decade, considerable efforts have been devoted in the design and the preparation of PNIPAAm-based thermosensitive polymeric micelles as delivery vehicles for controlled drug release.<sup>3–7</sup> There are two categories of PNIPAAm-based copolymer micelles as smart drug delivery systems, i.e., micelles with PNIPAAm as hydrophilic shell-forming segments below the LCST and micelles with PNIPAAm as hydrophobic core-forming segments above the LCST.<sup>8</sup>

Chitosan (CTS) is a popularly studied natural polysaccharide and is known for its plentiful resources, biocompatibility,

© 2012 Wiley Periodicals, Inc.

biodegradability, and reactivity for its free amine groups along its chains. These properties make CTS a good candidate for the development novel drug delivery systems. Graft copolymerization onto CTS via its amino or hydroxyl groups has been an effective way to achieve versatile molecular designs and enlarge the field of the potential applications of CTS. CTS also have the pH-sensitive properties due to the protonation–deprotonation equilibrium of free amino groups. The combination of CTS and PNIPAAm allows in new possibilities to develop carriers that simultaneously exhibit the properties of both components. Many studies concerning PNIPAAm/CTS dual responsive hydrogels have been reported. Chen et al.<sup>9</sup> prepared PNIPAAm/CTS semi-interpenetrating hydrogel particles acting as a controlled release vehicle for cyclic adenosine 3',5'-monophosphate. Cao et al.<sup>10</sup> synthesized PNIPAAm-CTS copolymers and investigated its potential for ocular gel-forming system. Tourrette et al.<sup>11</sup> incorporated PNIPAAm/CTS microgel onto plasma functionalized cotton fiber surface used as a novel responsive material. Lie et al.<sup>12</sup> and Fan et al.<sup>13</sup> obtained pH sensitive PNIPAAm/CTS nanoparticles loading paclitaxel and camptothecin by controlling the crosslinking degrees and reaction conditions. However, we note that the fine structures of the PNIPAAm-CTS copolymer or the hydrogel or the microgel were various attributing to the initiators, monomer concentrations, and crosslinker concentrations. The temperature-induced reversible self-assembly has not clearly been clarified. Besides, the effect of CTS molecular weight (Mw) on the final modified polymer still received little attention.

Herein, we prepared a series of double hydrophilic CTS-g-PNIPAAm copolymers using ammonium persulfate (APS) as initiator by solution polymerization from different Mw CTS. The grafting ratio (GR) and grafting efficiency (GE) increased with CTS Mw increasing. All the copolymers owned the similar LCST of 33.5°C, which was independent to the CTS Mw. Moreover, once the Mw of CTS increased to 200 kDa, the copolymers become less sensitive to the temperature. Dynamic laser scattering (DLS) method showed that the copolymers were less pH sensitive, when the Mw of CTS increased to 700 kDa, especially from pH 7.4 to 6.8. The copolymers could form uniform nanoparticles only if the temperature increased to 34°C reversibly. Results from DLS revealed that the copolymer crosslinked by GA and GP had a smaller size and more uniform polydispersity index (PDI). After crosslinked by *N,N*-methylenebisacrylamide (MBA), the structure of nanoparticles could be frozen. Surface tension method indicated that critical aggregate concentrations (CACs) of nanoparticles decreased from 0.045 to 0.036 mg mL<sup>-1</sup> prepared from CTS 50 to 700 kDa. From the above results, we think the most preferable Mw range of CTS for the modification are from 50 to 200 kDa, which can be sensitive to both the temperature and pH. On the contrary, structurally stable nanoparticles, which were more resistance to the dilution of serum were prepared by CTS with Mw more than 700 kDa. The Mw less than 50 kDa and more than 700 kDa were not covered in this article.

## MATERIALS AND METHODS

### Materials

CTS (degree of deacetylation, >90%, Mws approximately 50, 100, 200, and 700 kDa) was obtained from Zhejiang Jinke biochemical

(China). MBA was purchased from Sigma-Aldrich. NIPAAm was purchased from international laboratory (99%) and recrystallized in *n*-hexane, and APS was obtained from the product of ES. Genipin (GP) was purchased from Aladdin Chemistry Company. All the other chemicals were of analytical grade or above and used as received without further purification.

### Preparation of CTS-g-PNIPAAm Copolymers

Specified amount of CTS (0.2 g) with different Mws were dissolved in 20 mL 4% (v/v) acetic acid solution containing specific amount of NIPAAm (0.8 g).<sup>13–15</sup> The solution was purged with nitrogen and heated to 80°C for 30 min. Then, APS was dissolved in 5 mL of distilled water and purged into the solution. After 3.5–4 h of reaction, a solution containing CTS-g-PNIPAAm copolymers and PNIPAAm homopolymers were obtained. The dispersion was further purified by placing it into a dialysis bag with a 14,000-Da Mw cut-off (Viskase) and dialyzed against 5 L of deionized water for 48 h at room temperature (RT) to remove small molecules and unreacted monomers. Then the products were washed in methanol to remove homopolymers. The solution was then lyophilized and stored at desiccator before further study.

The GR and GE were calculating by the gravimetric analysis using the following equation:

$$GR = (W_1 - W_c) / W_c$$

$$GE = (W_2 - W_c) / W_c$$

In the equation,  $W_c$  is the initial weight of CTS.  $W_1$  is the primary weight of the products.  $W_2$  is the final weight of purified products.

**FTIR and 1H-NMR Spectroscopy Measurements of Copolymers.** Fourier transform infrared (FTIR, Thermo Nicolet Avetar 370) and 1H-nuclear magnetic resonance (1H-NMR, Bruker303K AV-500) measurements were used to investigate the chemical structure of CTS and CTS-g-PNIPAAm. The freeze-dried product was mixed with the KBr and compressed into disc to record the infrared (IR) spectra. Meantime, the copolymer was dissolved in D<sub>2</sub>O to record NMR spectrum.

**The Influence of Mw of CTS on the Size of Copolymer and LCST.** The freeze-dried products were reconstituted into aqueous solution (1.5 mg mL<sup>-1</sup>) and divided into two parts.<sup>16</sup> Part one is to measure the size of copolymer at 25°C and self-assembled polymeric nanoparticles at 37°C by DLS (Brookhaven instrument corporation, model: BI-APD) with a laser light wavelength of 532 nm at a 90° scattering angle. The Z-average hydrodynamic diameters of the particles were intensity-based mean diameter and given by the instrument directly calculated from correlation equation. Part two of the solution was subjected to observe transmission changes at 500 nm at designed temperature (25, 32, 32.5, 33, 33.5, 34, 34.5, 35, 37, and 40°C) by UV–vis spectrometer (Thermo scientific varioskan flash spectral scanning multimode reader). The samples were allowed to equilibrate for 10 min at each temperature before the measurements were taken.<sup>17</sup> In this study, the LCST of the resultant solution is defined as optical transmittance of the solution at 500 nm exhibiting inflexion due to PNIPAAm phase transition with the temperature.

**Studies on the pH-Dependent Size Change of Polymeric Nanoparticles.** The pH-sensitivity of resultant products was evaluated by detecting the size changes at different phosphate buffer

solutions (PBS). The copolymers were dissolved in PBS with different pH values (i.e. 5.0, 6.0, 6.8, 7.4, and 8.0), and the size of the nanoparticles were detected by a Zetasizer 3000HS instrument (Malvern Instruments, Malvern, UK) with 633 nm He-Ne lasers at 25°C after stirring.

### Studies on the pH Sensitivity of Copolymers by Fluorescence

**Probe Method.** In our study, pyrene fluorescence probe method was first used to investigate the changes of microenvironment of copolymer in PBS. Briefly, the same amount of polymers were added into the volumetric flasks containing acetone-free pyrene with final concentration of  $6 \times 10^{-7}$  M and the solutions were diluted with PBS with different pH. Then, the solutions were sonicated for 30 min followed by incubation at 40°C water bath for 1 h and kept from light overnight at RT. Fluorescence spectra were recorded with an RF-5301 PC fluorescence spectrophotometer (Shimadzu, Kyoto, Japan) with the emission wavelength at 390 nm. The slit widths for emission and excitation were set at 3.0 and 1.5 nm, respectively. The peak height intensity ratio (I3/I1) of the third peak (I3 at 338 nm) to the first peak (I1 at 333 nm) against temperature was plotted in PBS.

### Preparation of Core or Shell Crosslink Nanoparticles

Different types of crosslinkers were used to crosslink the internal core or shell of copolymer prepared from CTS with a  $M_w$  of 200,000. Two kinds of crosslinkers, GA (2%)<sup>18,19</sup> and GP (2%)<sup>20,21</sup> were added to the solution of copolymer ( $1.5 \text{ mg mL}^{-1}$ ) at 32°C for 24 h and then heated to 40°C for 2 h to consolidate the shell of micelle, respectively. The core crosslink products were prepared by the initially adding MBA before the reaction.<sup>12,13</sup>

**The Influence of Temperature on the Size of the Core Crosslink and Shell Crosslink Nanoparticles.** The hydrodynamic diameter and size distribution of the synthesized copolymers with or without crosslinking were measured by DLS method at 25, 32, 33, 34, 35, 37, and 40°C, respectively.

**Particle Size and Morphology Observation of Core Crosslink Nanoparticles.** The hydrodynamic diameter of core crosslink nanoparticles were observed by DLS. The morphologies of the CTS-PNIPAAm nanoparticles were observed by Transmission electron microscope (TEM) (Hitachi TEM, HC-1, 80 kV) and Atomic force microscopy (AFM) (Veeco NanoScope V, model: RTESP). Briefly, for TEM, a drop of the resultant nanoparticles solution containing 0.01% (w/v) phosphotungstic acid was placed on a copper grid coated with carbon film and air-dried at 20°C. For AFM, commercially available standard silicon probes with spring constant of  $40 \text{ N m}^{-1}$  and a tip radius of 7 nm (PPP-NCH, Nanosensors, and Switzerland) were used for imaging. The images were processed and analyzed using the Nanoscope software v5.30r3 (Veeco, Santa Barbara, CA). The sample preparation was similar to that for TEM ignoring negative staining, but silicon was used as substrate. The silicon substrate was washed with absolute ethanol and dried at RT.

**Table I.** Grafting Ratio and Grafting Efficiency of Copolymers

$M_w$ of CTS	50 kDa	100 kDa	200 kDa	700 kDa
GR (%)	3.115	3.799	3.822	11.951
GE (%)	0.552	0.893	0.904	4.956

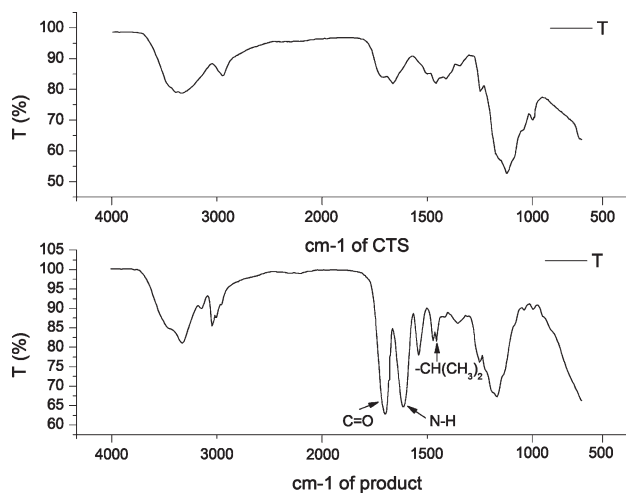


**Figure 1.** FTIR spectra of (a) CTS and (b) CTS-g-PNIPAAm.

**CAC of Structurally Permanently Nanoparticles.** The CAC was determined by surface tension method. Briefly, different amounts of polymers were added into the volumetric flasks, and the final polymer concentrations were ranged from  $1.5 \times 10^{-3}$  to  $1.5 \text{ mg mL}^{-1}$ . The polymer solutions were measured by Dataphysics DCAT21 to record the surface tension at the interface at 25°C. In this work, the surface tension was measured as a function of the concentration of polymers, and the CAC was calculated as the inflection point of the  $\gamma$ -lnC plot.<sup>22,23</sup>

## RESULTS AND DISCUSSION

### Preparation of CTS-g-PNIPAAm Copolymers

Both GR and GE results were shown in Table I. With the increase of  $M_w$  of CTS, GR and GE takes on ascend trend.

Figure 1 showed the FTIR spectra of original CTS and typical CTS-g-PNIPAAm copolymer with CTS  $M_w$  200 kDa. In comparison with the original CTS, the characteristic peaks at  $1589 \text{ cm}^{-1}$  for  $-\text{NH}_2$  of CTS and  $2876$  and  $1375 \text{ cm}^{-1}$  for single  $\text{CH}_3-$  of CTS disappeared, for CTS-g-PNIPAAm copolymer, while two new peak occurred at  $1536$  and  $1458 \text{ cm}^{-1}$ , suggesting that  $-\text{NH}_2$  of CTS might be transformed into C-N bond

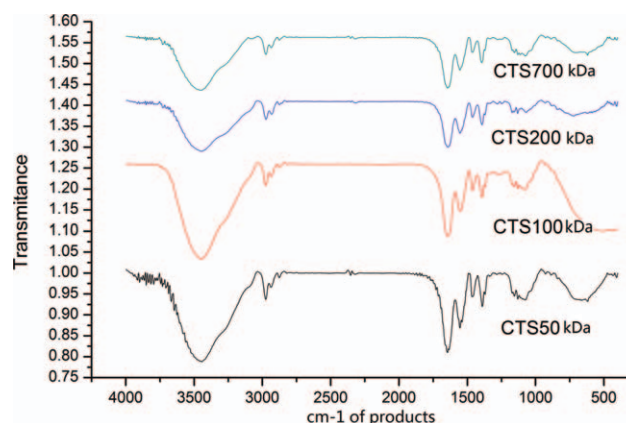


**Figure 2.** FTIR spectra of a series of CTS-g-PNIPAAm copolymers. [Color figure can be viewed in the online issue, which is available at [wileyonlinelibrary.com](http://www.intelibrary.com).]

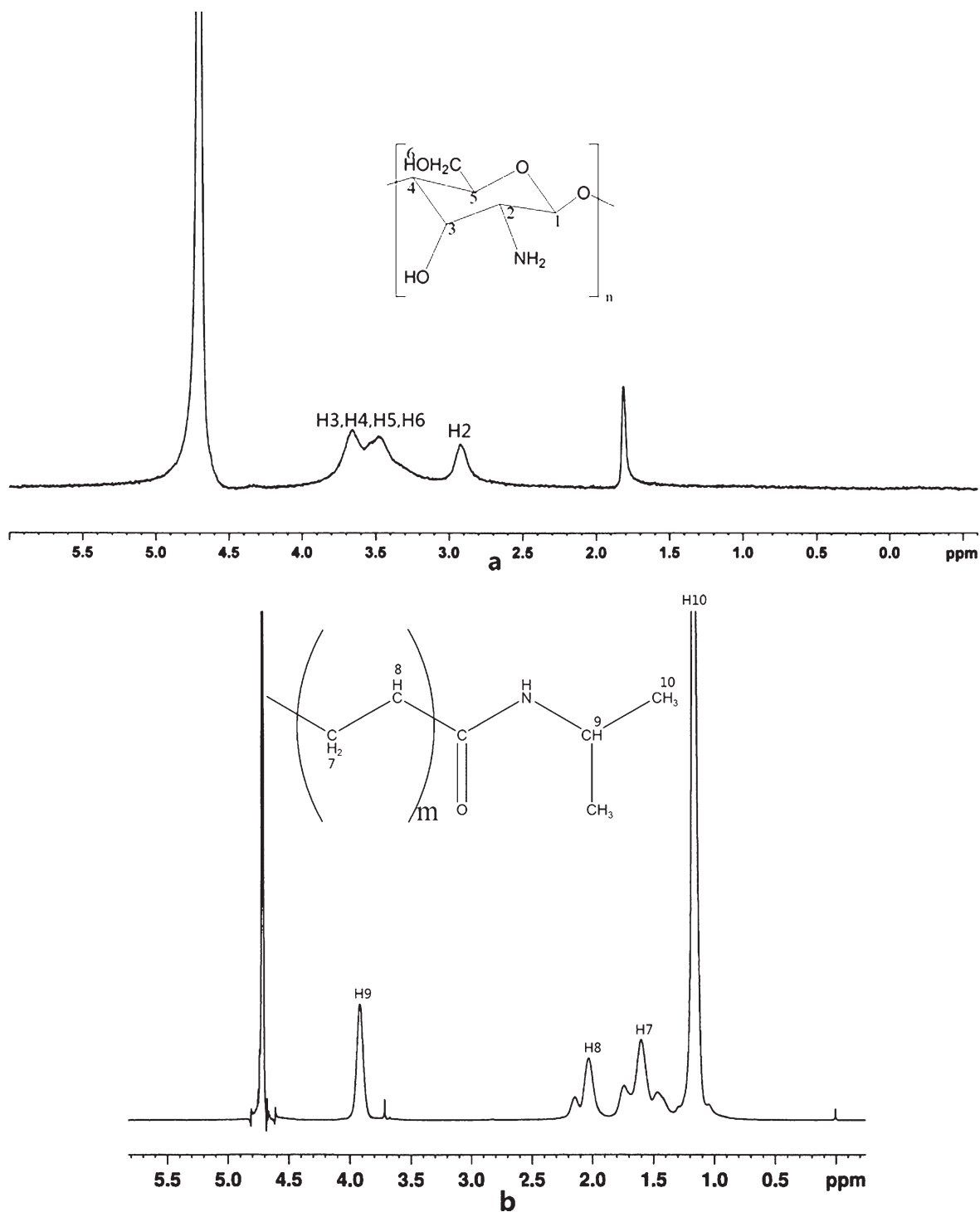


Figure 3. <sup>1</sup>H-NMR spectra of (a) CTS and (b) CTS-g-PNIPAAm.

and N—H bond. At the same time, the characteristic peaks at 1386 and 1367  $\text{cm}^{-1}$  for isopropyl group and 1630  $\text{cm}^{-1}$  ( $\text{O}=\text{C}$ ) showed the presence of PNIPAAm. Figure 2 showed a series of FTIR spectra prepared by CTS with different  $M_w$ . The copolymers showed similar spectra. Moreover, as the increasing  $M_w$  of CTS, the absorption peak intensity in 1630  $\text{cm}^{-1}$  ascribed to carbonyl group decreased. The results from IR spectra were in dis-

agreement with the results from calculation from GR and GE, apparently. The fact is only mass gain is concerned when calculating the GR and GE, ignoring the effect of CTS  $M_w$ .

A typical <sup>1</sup>H-NMR spectrum of CTS and copolymer with CTS  $M_w$  200 kDa was shown in Figure 3(a,b). The characteristic peaks at  $\delta = 0.82\text{--}2.10$  ppm and 3.66–3.82 ppm in Figure 3(b)



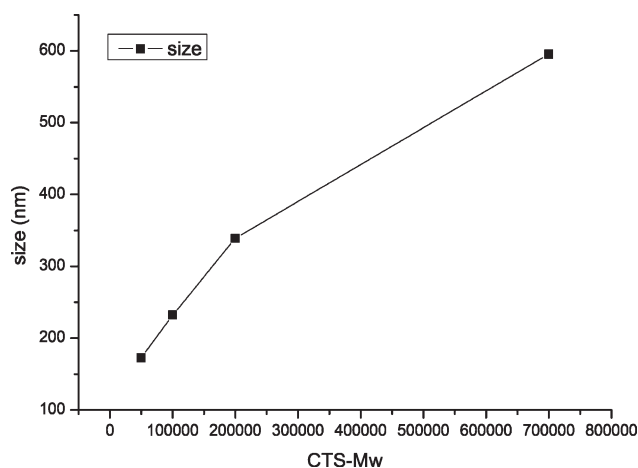


Figure 4. Effect of Mw of CTS on the size of CTS/PNIPAAm copolymers.

were observed for the protons of PNIPAM, indicating that PNIPAM was grafted into the bone of CTS successfully. These results further demonstrated the successful preparation of CTS-g-PNIPAAm copolymer and could dissolve in D<sub>2</sub>O at 25°C.

Recently, the ability to prepare precursor macromolecules of well-defined structure and architecture has been substantially enhanced by the in situ radical polymerizations. It is well known that the radical polymerization reaction can be initiated by different methods. Chuang et al.<sup>24</sup> initiated this reaction by cerium ammonium nitrate to prepare PNIPAAm/CTS copolymers. Lee and Chen<sup>25</sup> synthesized the crosslinked poly(NIPAAm-CTS) complex particles by APS. Li et al.<sup>12</sup> and Fan et al.<sup>13</sup> prepared poly NIPAAm/CTS nanoparticles using *tert*-butyl hydroperoxide as initiators. In this study, strong oxidizer APS was used to generate activated radical in the backbone of CTS, especially in C2 and free amine group to initiate the reaction, the double bond of NIPAAm monomer opened and polymerized to form grafted copolymer with CTS as the main chain and PNIPAAm as branched building block. We thought APS can initiate the reaction with a good reproducibility compared with others. Meantime, the products prepared by a higher Mw CTS could be separated by acetone precipitation, on the contrary, by a lower Mw CTS could not. We finally selected dialysis method to purify the product to ensure homogeneous reaction conditions.

#### The Influence of Mw of CTS on the Size of Copolymer and LCST

It is well known that the micellar nanoparticles self-assembling behavior from graft copolymer were closely related to the Mw of single block and by simply adjusting the hydrophobicity/hydrophilicity of the modified CTS chain, stable nanoparticles could be obtained directly. In this study, we synthesized a series of CTS-g-PNIPAAm copolymers and observed the effects of CTS Mw on the size of final products below and above the LCST.

Figure 4 showed the mean diameter of copolymer prepared from different Mw CTS at RT, and the mean diameter of copolymer in water grew up gradually with the increase of Mw of CTS. Huang et al.<sup>26</sup> used different Mw CTS to delivery DNA

and reported that the mean particle size decreased from 181 to 155 nm when the CTS Mw fell from 213 to 48 kDa. We possessed a more obviously ascending trend. We speculated that our copolymers were soluble in water and the molecular chains were in a stretched state. Therefore, the Mws have a more obvious effect on size from 173 to 595 nm with the CTS Mw increased from 50 to 700 kDa. However, PDIs, which measured the width of size distributions, were all up to 1, which shows that the copolymer could not self-assemble successfully at RT.

Figure 5 showed the variances of absorbance of different copolymers at designed temperatures. All the resultant copolymers showed the similar "LCST," which was near 33.5°C. So the conclusion could be made that the thermosensitive characteristic of the resultant copolymer was independent to the CTS Mw, and this may attribute to the facts that the thermosensitive characteristics depended on the block of PNIPAAm, while the same synthesis method and monomer weight of NIPAAm were used. Our results were in good agreement with Fujishige et al.,<sup>27</sup> who reported that the LCST of PNIPAAm was independent of the Mw and the concentration, but could be changed upon shifting the hydrophilic/hydrophobic balance. Moreover, when the CTS Mw increased to 200 kDa, we found the products were less sensitive to temperature than the products synthesized by CTS with lower Mw. This may be due to the increased viscosity of CTS with the higher Mws, which may prevent the molecular chain extension freely and prevented the approaching of activated monomer.

#### Studies on the pH-Dependent Size Change of Blank Polymeric Nanoparticles

Figure 6 showed that the copolymers from CTS with different Mw possessed the similar pH responsive behavior in different PBS, which was above the pH 7.4, mean hydrodynamic size was smaller, and more importantly speaking, the PDI increased rapidly. We boldly supposed that below the pH 6.8, the structure of nanoparticles were condensed and had a tendency of repelling drugs out of hydrophobic regions. We think the resultant copolymers owned the similar pH-sensitive features and could be very sensitive to mild changes of pH in nearly neutral

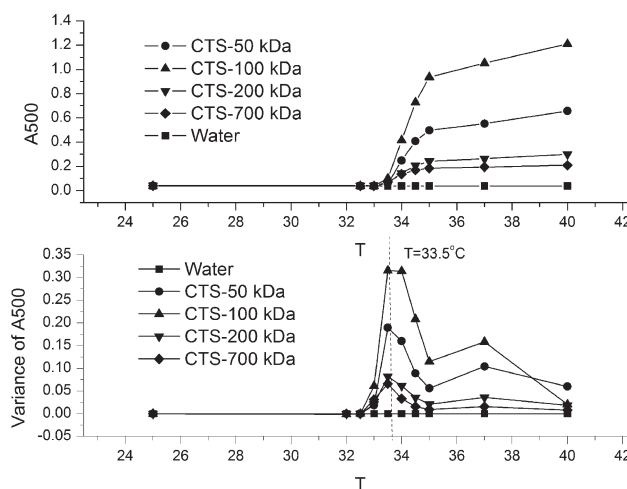


Figure 5. Effect of Mw of CTS on the LCST of CTS/PNIPAAm copolymer.

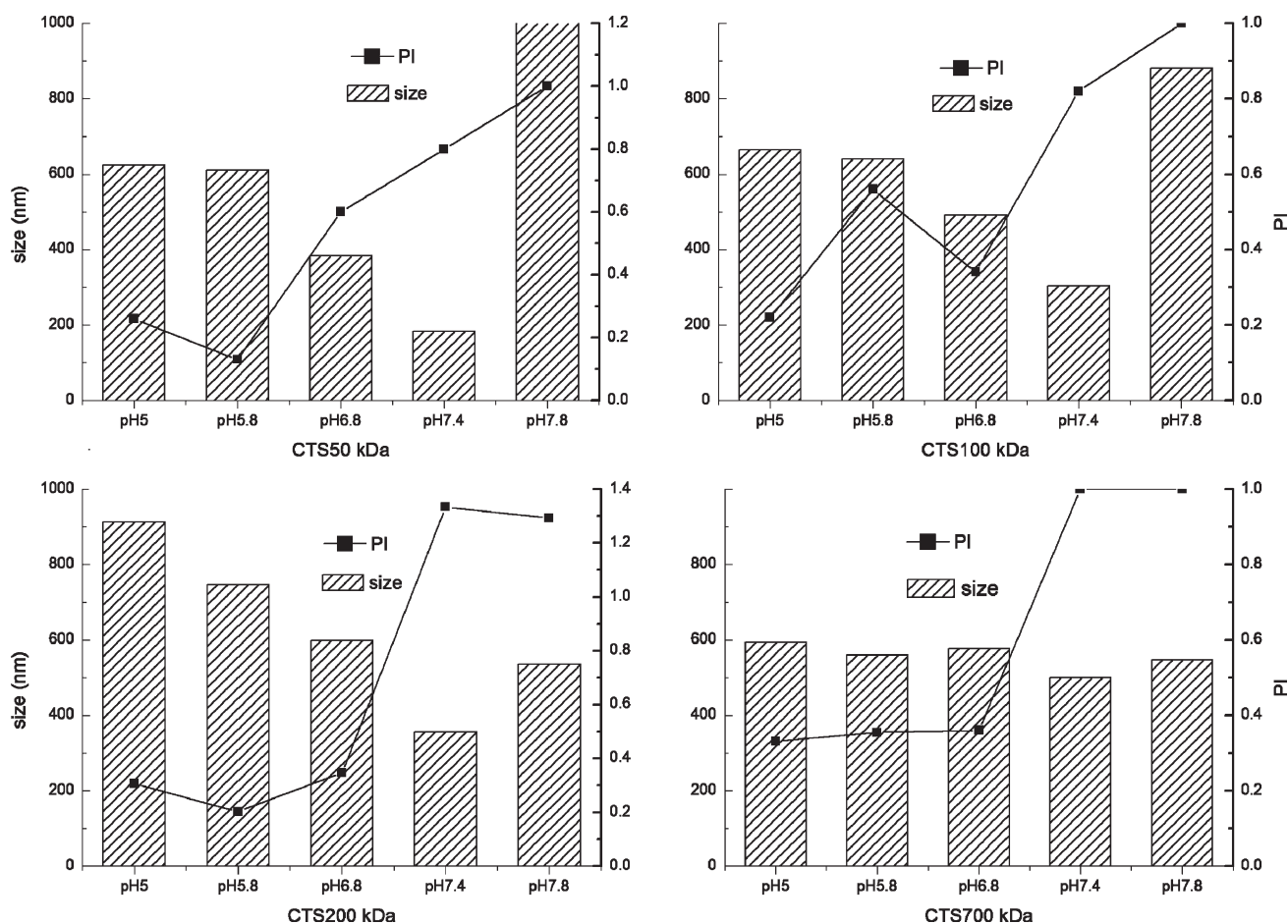


Figure 6. Mean size and poly diversity index of every products reconstituted in different pH PBS.

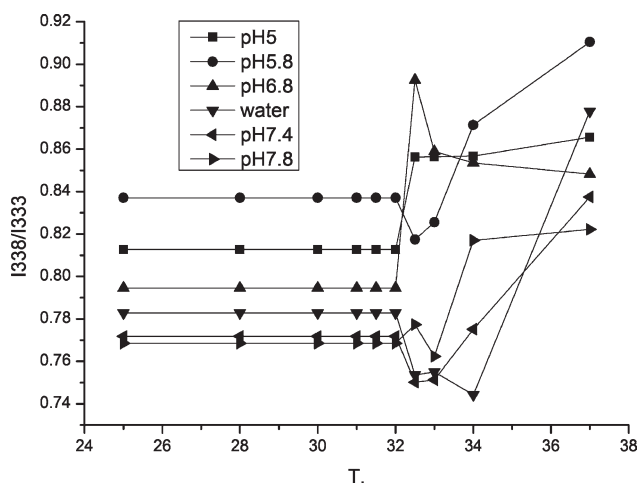
environment. Results in this study were in accordance with the Li et al.<sup>12</sup> and Fan et al.<sup>13</sup> reported that the similar nanoparticles could be very sensitive to the pH nearby the tumor site and may provide some practical and structural basis. It is commonly realized that the tumor microenvironment is more acidic than normal tissue<sup>28–30</sup> and may be used as the stimulus signal for drug release. Interestingly, when the Mw of CTS increased to 700 kDa, the pH-dependent size change disappeared although the trend for PDI kept the same. So, we studied the pH-dependent fluorescence behavior of copolymer prepared by CTS 200 kDa.

Figure 7 showed the representative plot of I338/I333 intensity ratio versus temperature in different PBS. It was found that the fluorescence intensity ratio possessed the reversed trend at pH 6.8 and 7.4 and at the temperature near the LCST. It is reported that I338/I333 ratio is proportional to the polar of microenvironment of pyrene.<sup>31</sup> We thought, first the copolymers were soluble in pH 7.4 solutions. When the temperature rose to above LCST, the PNIPAAm segment become hydrophobic and could solubilize the pyrene molecular for hydrophobic interactions. So, the curve dropped down first. But as the temperature continued to rise, the pyrene would be expelled from shrinking hydrophobic region, the I338/I333 ratio increased finally. We think that it provides the direct proof of CTS-g-PNIPAAm

structure changes caused by pH, which might provide some theoretical basis of the pH sensitivity of the copolymer.

#### Thermo-Dependent Self-Assembly of CTS-g-PNIPAAm Copolymers

This graft copolymer showed thermo-dependent self-assembly behavior in aqueous solution. That is, under LCST, the PNIPAAm of the polymer kept water-soluble and no nanoparticle was formed. As temperature increased to LCST, the phase transition that is from a hydrophilic state (random coil) to a hydrophobic state (globule and aggregation) related to PNIPAAm occurred.<sup>2,6,32</sup> Then these copolymers could form micellar-like nanoparticles. As DLS was proved to be a sensitive method to trace the formation of micellar-like nanoparticles according to the change in particle size and scattered light intensity.<sup>16</sup> The changes of micelle size and count rate with temperature changing were shown in Figure 8. The scattered light intensity was given here in kilo counts per second (kcps). It could be seen that the values of kcps were very small and kept unchanged under LCST, while the homogeneous size could not be measured. However, the kcps increased dramatically, when the temperature was increased above 34°C. The increase in count rate could be ascribed to a change in the refractive index of copolymer self-assembling into nanoparticles as its PNIPAAm block underwent a phase transition from random coil to condensed



**Figure 7.** I338/I333 of Mw 200 kDa prepared resultant product redissolving in PBS.

globule. The latter structure of PNIPAAm possessed higher refractive index than that of the former one. This change indicated clearly that the micelle began to form at around 34°C. According to the curve of count rate versus temperature, the critical micelle temperature was calculated to 34°C, which was in accordance with the results from the results of LCST.

#### Shell or Core Crosslink Products

The stability of the nanoparticles is an important issue because the thermoresponsive self-assembly is reversible in most of cases. To enhance the structural stability and integrity of the

supramolecular nanostructures formed by DHBCs, the strategies of covalent stabilization via crosslinking of the micellar core or shell were extensively explored. Moreover, it is reasonable to expect that the core crosslinked (CCL) or shell crosslinked micelles fabricated from DHBCs should possess stimuli-responsive cores or shells as well.<sup>33</sup> From the above results, it was known that the self-assembly only occurred at the temperature above LCST. However, the high stability of the micelles was crucial for clinical applications because the dissociation of micelles into individual polymer chains after administration might lead to rapid release of the entrapped drug, resulting in side effects in vivo. Several methods were chosen to consolidate the structure of nanoparticles formed to obtain permanent nanoparticles in this study.

GA, a usual crosslinker, was ever and widely used to crosslink CTS-based nanoparticles as the existence of free amine group on the back bone of CTS. Unfortunately, the toxicity of GA on cell viability limited its use in the field of drug delivery.<sup>34,35</sup> GP, an extract from plant gardenin, has been reported by many authors<sup>20,36,37</sup> that could effectively crosslink CTS and was proved to be more safe as a biocompatible crosslinker<sup>38,39</sup> compared with GA. However, the mechanism of crosslink is unclear. Both GA and GP were selected to crosslink the hypothetical CTS shell. After the reaction, the yellow and blue solutions were obtained, crosslinked by GA and GP, respectively. Meanwhile, MBA was a commonly used crosslinker for PNIPAAm, which could change the liner polymer into three-dimensional polymer due to its double functional groups; it was selected to crosslink the PNIPAAm core. After the reaction, a solution with weak opalescence was obtained.

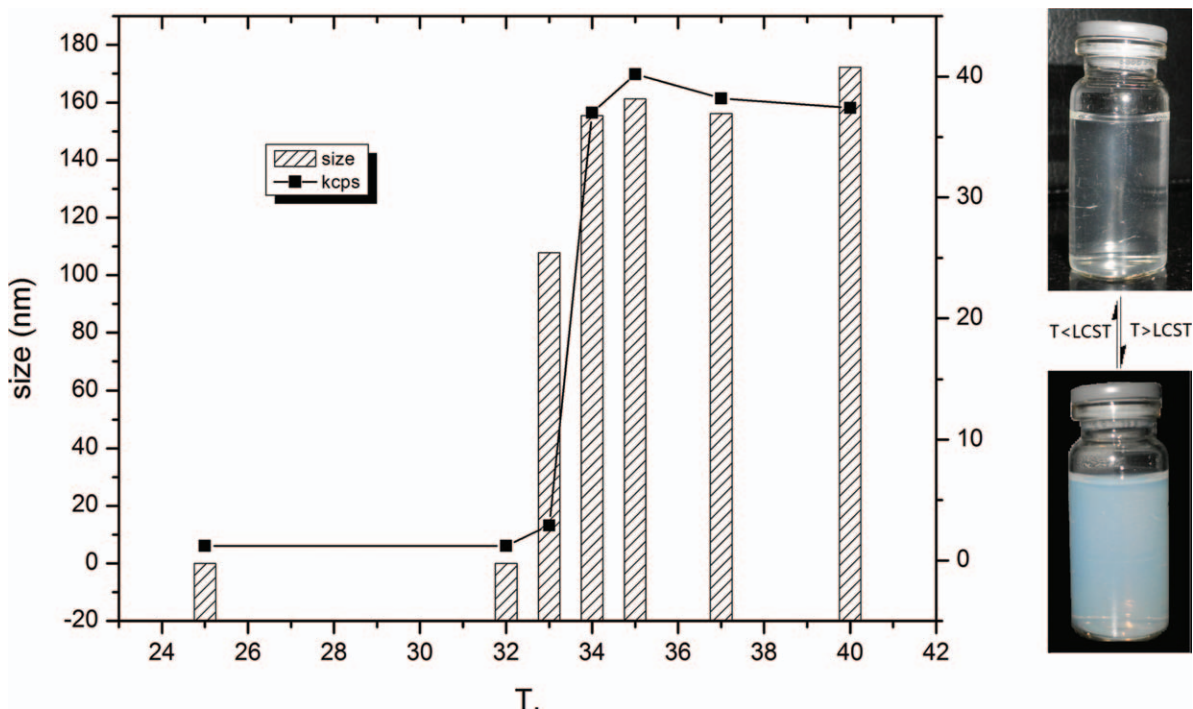


**Figure 8.** Micelle size and scattered light intensity of copolymer synthesized from CTS200 kDa as a function of temperature in water. Total concentration of the system is 1.5 mg mL<sup>-1</sup>. [Color figure can be viewed in the online issue, which is available at [wileyonlinelibrary.com](http://wileyonlinelibrary.com).]

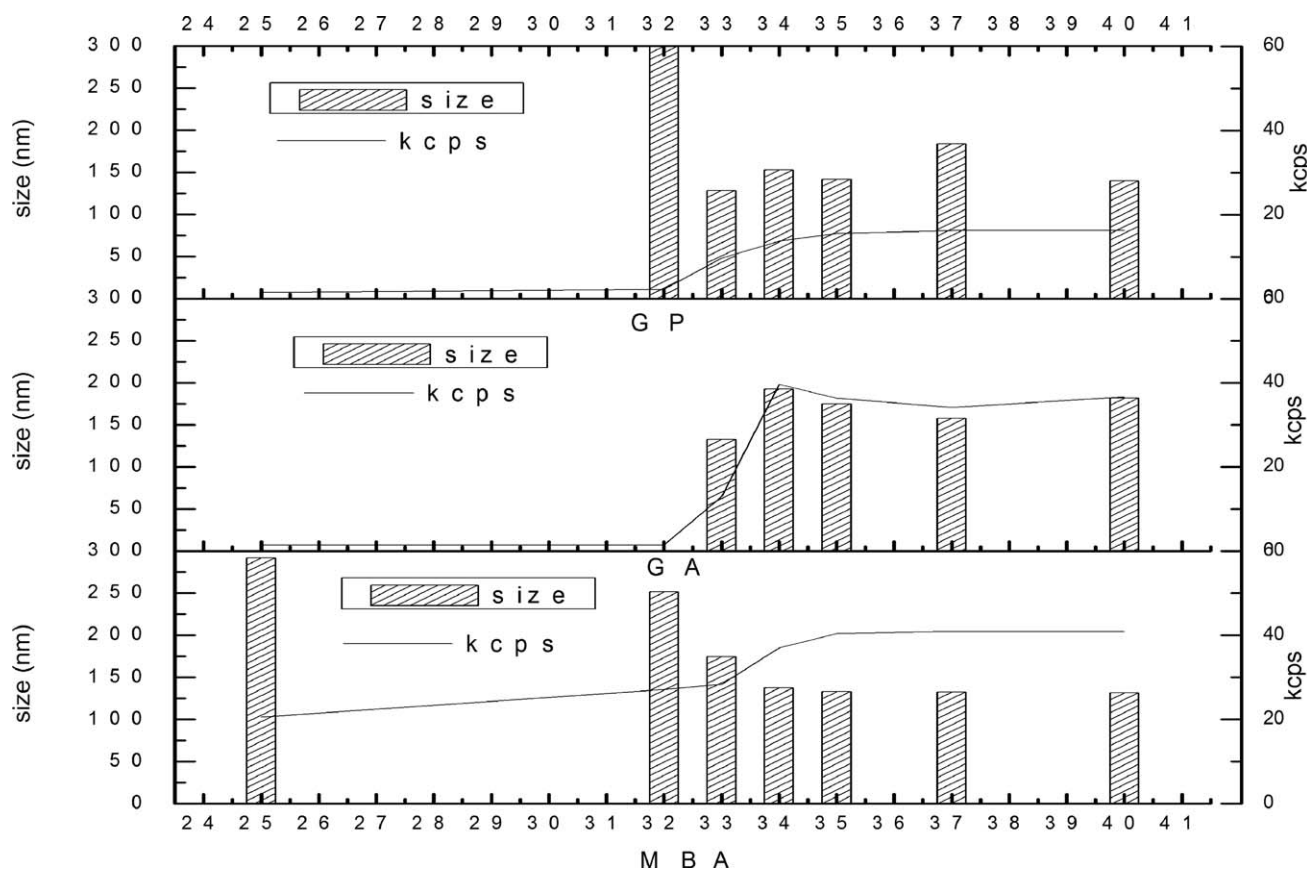


**Figure 9.** Micelle size and scattered light intensity of crosslinked copolymer by (a) GA, (b) GP, and (c) MBA synthesized from CTS200 kDa as a function of temperature in water.

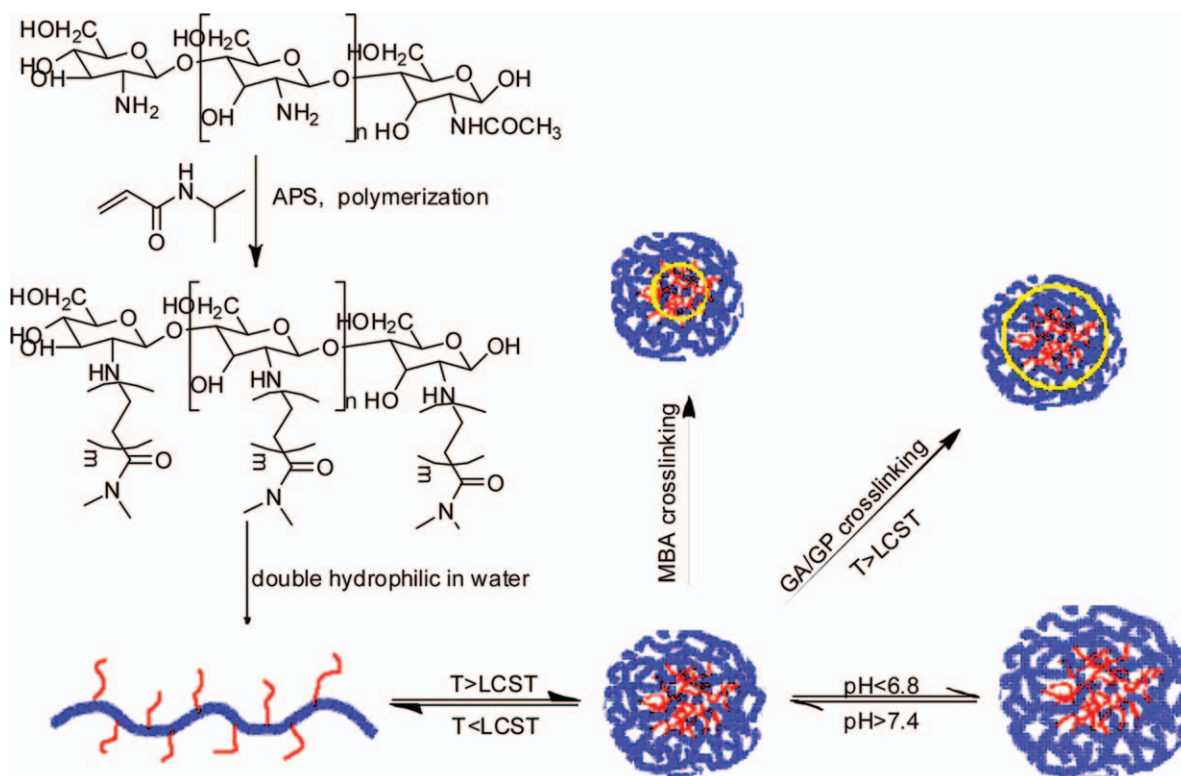


**Figure 10.** Illustration of structures of CTS-g-PNIPAAm copolymer and responsive self-assembly behaviors. [Color figure can be viewed in the online issue, which is available at [wileyonlinelibrary.com](http://wileyonlinelibrary.com).]



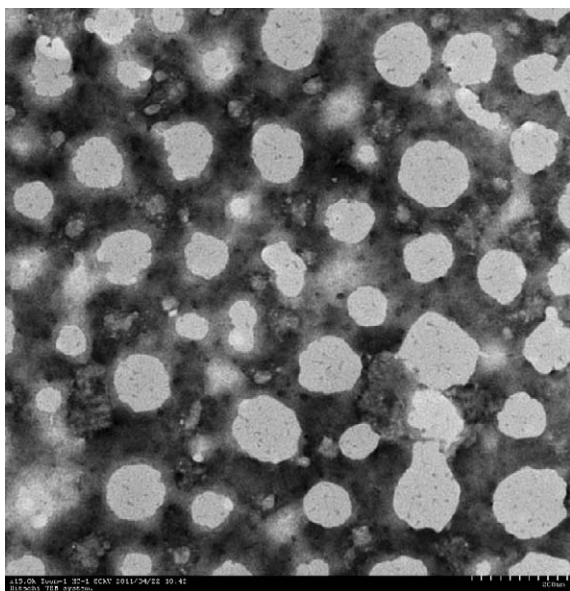


Figure 11. TEM of MBA crosslink nanoparticles.

The same DLS was used to observe the formation and variation of the core or shell crosslink products. From Figure 9, it was found that the products resulted from the GA or GP crosslinking kept or even improved its original thermosensitivity com-

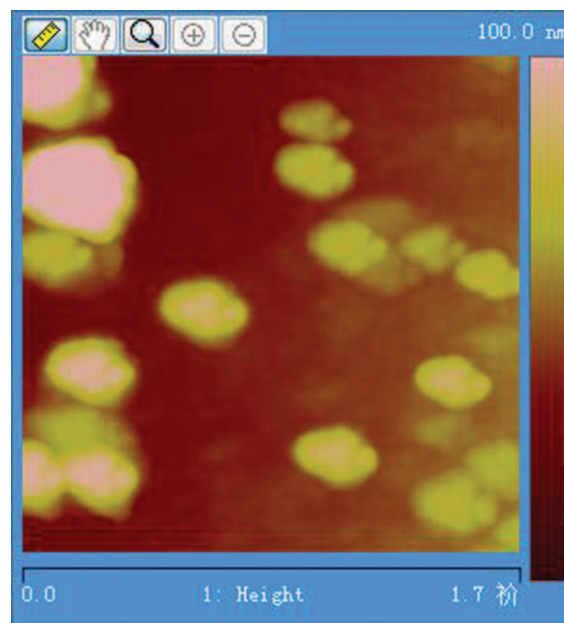


Figure 12. AFM of MBA crosslink nanoparticles. [Color figure can be viewed in the online issue, which is available at [wileyonlinelibrary.com](http://wileyonlinelibrary.com).]

pared with the product without crosslinking. While polymer crosslinked by MBA not only kept its original thermosensitivity

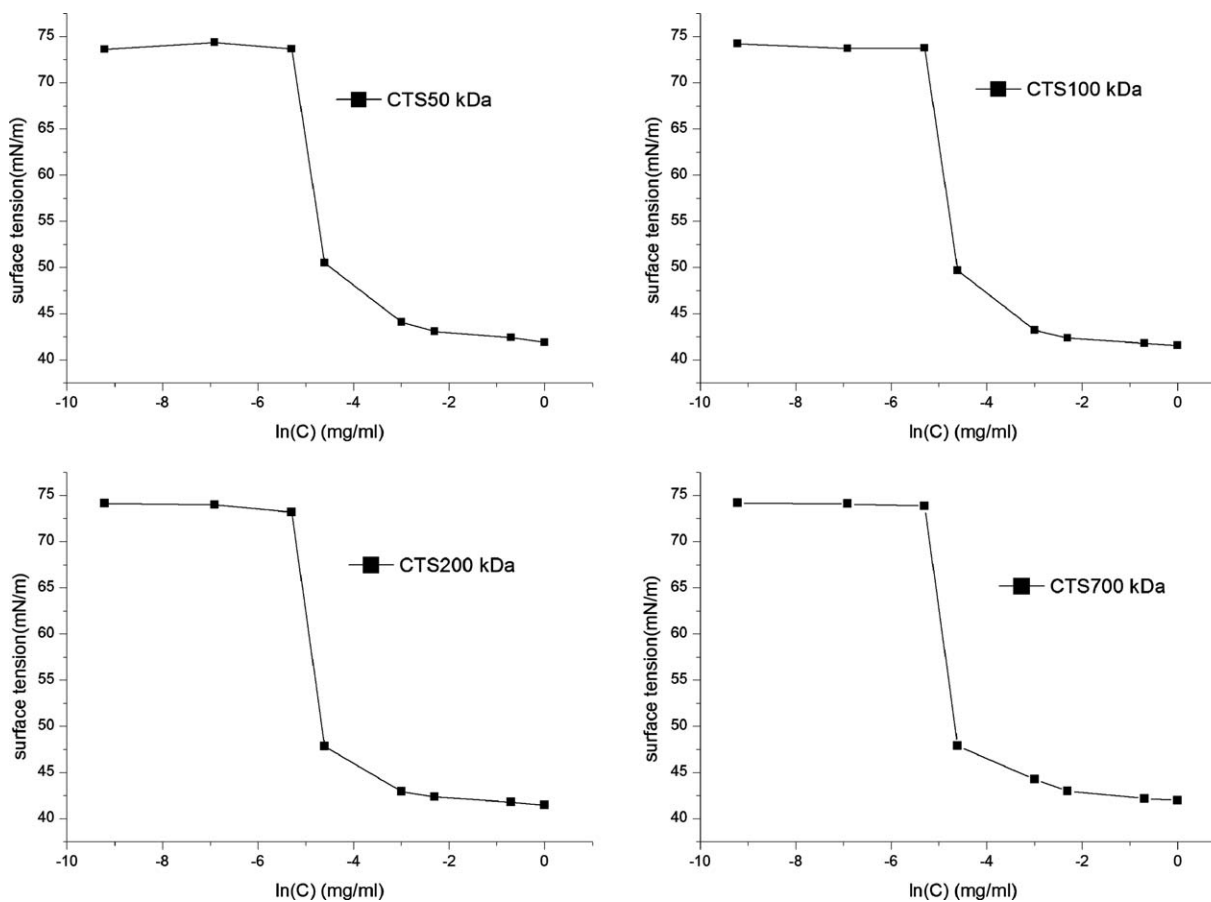


Figure 13. The plot of surface tension versus Ln(C) in water at RT of crosslinked nanoparticles prepared from CTS with Mw 50, 100, 200, and 700 kDa.

**Table II.** CAC (mg mL<sup>-1</sup>) of Products Prepared by Different Mw of CTS

Mw of CTS	50 kDa	100 kDa	200 kDa	700 kDa
CAC (mg mL <sup>-1</sup> )	0.045	0.042	0.037	0.036

but also can form permanent nanoparticles whose formation is independent to the temperature. However, in this study, the structurally stable nanoparticles were not obtained after cross-linked by GA and GP. The temperature-dependent self-assembly was still tunable. It was speculated that because most of the active amine group at the backbone of CTS had reacted with PNIPAAm, leading to decreased crosslink efficiency. On the contrary, precrosslinking with MBA combined with reasonable monomer quantity control, we could obtain stable nanoparticles that differ from the former interpenetrating polymer network (IPN) hydrogel structure<sup>17,40,41</sup> and have great potential in drug delivery. Moreover, it was found that after crosslinking by GA or GP, the nanoparticles possessed a more preferable PDI. The plots of mean size and kcps of crosslinked copolymer (a) by GA, (b) by GP, and (c) by MBA synthesized from CTS 200,000 as a function of temperature in water were shown in Figure 9 with a total concentration of 1.5 mg mL<sup>-1</sup>. The graphic abstract was shown in Figure 10.

#### TEM and AFM of Core Crosslink Products

Figure 11 showed the representative TEM micrograph of the nanoparticles formed from CCL by MBA, which was spherical with a narrow size distribution. These dense dark nanoparticles were well dispersed as individual. This was due to the action of the staining agent, phosphotungstic acid, which could penetrate into the inner cores for its unconsolidated structure formed from polysaccharide modified polymer. The size obtained from TEM (50–100 nm) was smaller than that observation from DLS (100–150 nm). This could be related to the fact that DLS measures the hydrodynamic diameter of the micelles in an aqueous environment, whereas the TEM micrograph showed the dehydrated solid state of the nanoparticles formed from CCL by MBA.

The size and shape of the nanoparticles were further measured in the solid state by AFM as shown in Figure 12. The AFM observation gave the mean diameter around; these results were consistent with that observed from TEM.

#### Critical Aggregate Concentration

The surface tension method is widely used by many authors<sup>42,43</sup> to investigate the CAC of the micellar-like nanoparticles for their decreasing surface tension effects. Figure 13 showed the surface tension as a function of polymer concentration. Table II showed the CAC values for the different products. The CAC value decreased from 0.045 to 0.036 mg mL<sup>-1</sup>, when the CTS Mw increased from 50 to 700 kDa. Öping-Höggård et al.<sup>44</sup> observed the effect of CTS Mw as gene carrier. The results showed that high Mw CTS were superior to those with low Mw in enhancing the stability of complexes, which is beneficial for the protection of DNA in the cellular endosomal/lysosomal compartments. Our results were in accordance with them. The crosslinked nanoparticles synthesized by CTS with lower Mw were less stable acting as intravenous drug carriers. Thus, our research enriched the study of CTS modification as drug nanocarrier.

## CONCLUSION

In this article, we prepared a series of CTS-g-PNIPAAm copolymers and studied the effect of CTS Mw on self-assembly behavior of copolymers. The copolymers possessed the similar LCST, which was near 33.5°C and could form uniform nanoparticles only if the temperature increased to 34°C reversibly. After cross-linked by MBA, structurally stable nanoparticles were obtained, which kept the original thermosensitive character. We thought the most preferable Mw range of CTS for modification is from 50 to 200 kDa, which can be sensitive to both the temperature and pH especially from pH 6.8 to 7.4. In addition, structurally stable nanoparticles, which were more resistance to the dilution of serum, were prepared by CTS with Mw over than 700 kDa. It was suspected to be a potential anticancer drug carrier.

## ACKNOWLEDGMENTS

This study was supported by National Natural Science Foundation of China (No. 81001412) and Research Special Fund for Central University (No. JKQ2009006).

## REFERENCES

- Cölfen, H. *Macromol. Rapid Commun.* **2001**, *22*, 219.
- Schild, H. *Prog. Polym. Sci.* **1992**, *17*, 87.
- Xiong, W.; Wang, W.; Wang, Y.; Zhao, Y.; Chen, H.; Xu, H.; Yang, X. *Colloids Surf. B Biointerfaces*, **2011**, *84*, 447.
- Kono, K.; Henmi, A.; Yamashita, H.; Hayashi, H.; Takagishi, T. *J. Control. Release* **1999**, *59*, 63.
- Fu, G.; Soboyejo, W. O. *Mater. Sci. Eng. C* **2011**, *31*, 1084.
- Eeckman, F.; Moës, A. J.; Amighi, K. *Int. J. Pharm.* **2004**, *273*, 109.
- Chung, J. E.; Yokoyama, M.; Yamato, M.; Aoyagi, T.; Sakurai, Y.; Okano, T. *J. Control. Release* **1999**, *62*, 115.
- Wei, H.; Cheng, S.-X.; Zhang, X.-Z.; Zhuo, R.-X. *Prog. Polym. Sci.* **2009**, *34*, 893.
- Chen, X.; Song, H.; Fang, T.; Bai, J.; Xiong, J.; Ying, H. *J. Appl. Polym. Sci.* **2010**, *116*, 1342.
- Cao, Y.; Zhang, C.; Shen, W.; Cheng, Z.; Yu, L.; Ping, Q. *J. Control. Release* **2007**, *120*, 186.
- Tourrette, A.; De Geyter, N.; Jovic, D.; Morent, R.; Warmoeskerken, M. M. C. G.; Leys, C. *Colloids Surf. A Physicochem. Eng. Asp.* **2009**, *352*, 126.
- Li, F.; Wu, H.; Zhang, H.; Li, F.; Gu, C.-h.; Yang, Q. *Carbohydr. Polym.* **2009**, *77*, 773.
- Fan, L.; Wu, H.; Zhang, H.; Li, F.; Yang, T.-h.; Gu, C.-h.; Yang, Q. *Carbohydr. Polym.* **2008**, *73*, 390.
- Lee, C.-F.; Wen, C.-J.; Chiu, W.-Y. *J. Polym. Sci. Part A Polym. Chem.* **2003**, *41*, 2053.
- Zhang, H.-f.; Zhong, H.; Zhang, L.-l.; Chen, S.-b.; Zhao, Y.-j.; Zhu, Y.-l. *Carbohydr. Polym.* **2009**, *77*, 785.
- Zhang, Z.-X.; Liu, K. L.; Li, J. *Macromolecules* **2011**, *44*, 1182.
- Cai, H.; Zhang, Z. P.; Chuan Sun, P.; Lin He, B.; Xia Zhu, X. *Radiat. Phys. Chem.* **2005**, *74*, 26.
- Ying, X.-Y.; Cui, D.; Yu, L.; Du, Y.-Z. *Carbohydr. Polym.* **2011**, *84*, 1357.

19. Wang, C.; Yang, F.; Zhang, H. *Separ. Purif. Technol.* **2010**, *75*, 358.
20. Muzzarelli, R. A. A. *Carbohydr. Polym.* **2009**, *77*, 1.
21. Mi, F.-L.; Tan, Y.-C.; Liang, H.-F.; Sung, H.-W. *Biomaterials* **2002**, *23*, 181.
22. Bell, C. G.; Breward, C. J. W.; Howell, P. D.; Penfold, J.; Thomas, R. K. *J. Colloid Interf. Sci.* **2010**, *350*, 486.
23. Ritacco, H.; Kurlat, D. H. *Colloids Surf. A Physicochem. Eng. Asp.*, **2003**, *218*, 27.
24. Chuang, C.-Y.; Don, T.-M.; Chiu, W.-Y. *Carbohydr. Polym.*, **2011**, *84*, 765.
25. Lee, W.-F.; Chen, Y.-J. *J. Appl. Polym. Sci.* **2001**, *82*, 2487.
26. Huang, M.; Fong, C. W.; Khor, E.; Lim, L. Y. *J. Control. Release* **2005**, *106*, 391.
27. Fujishige, S.; Kubota, K.; Ando, I. *J. Phys. Chem.* **1989**, *93*, 3311.
28. Tannock, I. F.; Rotin, D. *Cancer Res.* **1989**, *49*, 4373.
29. Maeda, H.; Bharate, G. Y.; Daruwalla, J. *Eur. J. Pharmaceut. Biopharmaceut.* **2009**, *71*, 409.
30. Lee, E. S.; Gao, Z.; Bae, Y. H. *J. Control. Release* **2008**, *132*, 164.
31. Capek, I. *Adv. Colloid Interf. Sci.* **2002**, *97*, 91.
32. Zhang, X.-Z.; Zhuo, R.-X. *Langmuir* **2000**, *17*, 12.
33. U. Kedar, P. Phutane, S. Shidhaye and V. Kadam, Nanomedicine: Nanotechnology, Biology and Medicine, **2010**, *6*, 714.
34. Zeiger, E.; Gollapudi, B.; Spencer, P. *Mutat. Res. Rev. Mutat. Res.* **2005**, *589*, 136.
35. Jayakrishnan, A.; Jameela, S. R. *Biomaterials* **1996**, *17*, 471.
36. Karnchanajindanun, J.; Srisa-ard, M.; Baimark, Y. *Carbohydr. Polym.* **2011**, *85*, 674.
37. Yuan, Y.; Chesnutt, B. M.; Utturkar, G.; Haggard, W. O.; Yang, Y.; Ong, J. L.; Bumgardner, J. D. *Carbohydr. Polym.* **2007**, *68*, 561.
38. Lau, T. T.; Wang, C.; Wang, D.-A. *Compos. Sci. Technol.* **2010**, *70*, 1909.
39. Pal, K.; Paulson, A. T.; Rousseau, D. In *Modern Biopolymer Science*; Stefan, K., Ian, T. N., Johan, B. U., Eds.; Academic Press: San Diego, CA, **2009**, p 519.
40. Chen, J.; Sun, J.; Yang, L.; Zhang, Q.; Zhu, H.; Wu, H.; Hoffman, A. S.; Kaetsu, I. *Radiat. Phys. Chem.* **2007**, *76*, 1425.
41. Guo, B.-L.; Gao, Q.-Y. *Carbohydr. Res.* **2007**, *342*, 2416.
42. Kjellin, U. R.; Reimer, J.; Hansson, P. *J. Colloid Interf. Sci.* **2003**, *262*, 506.
43. Jain, N.; Trabelsi, S.; Guillot, S.; McLoughlin, D.; Langevin, D.; Letellier, P.; Turmine, M. *Langmuir* **2004**, *20*, 8496.
44. Köping-Höggård, M. I. T.; Guan, H.; Edwards, K.; Nilsson, M.; Vårum, K. M.; Artursson, P. *Nature* **2001**, *8*, 14.